Int. J. Electrochem. Sci., 10 **(2015)** 6703 - 6713

International Journal of
ELECTROCHEMICAL
SCIENCE
www.electrochemsci.org

Preparation and Electrocatalytic Behavior of CoTPP/RGO Nanocomposite for Dioxygen Reduction

Guofang Zuo[1,*], *Qi Wang*[2], *Zhifeng Li*[1], *Jiandong Yang*[3], *Peng Wang*[1]

[1] College of Chemical Engineering and Technology, Tianshui Normal University, Tianshui 741000, P. R. China
[2] School of Chemical and Biological Engineering, Lanzhou Jiaotong University, Lanzhou 730070, P. R. China
[3] Department of Biology and Chemistry, Longnan Normal College, Chengxian 742500, P. R. China
[*]E-mail: zogofn@126.com

Received: 6 May 2015 / *Accepted:* 14 June 2015 / *Published:* 24 June 2015

In this paper, cobalt porphyrin combining with reduced graphene oxide (RGO) through an aromatic π-π stacking interaction made up a cobalt meso-tetraphenylprophyrin-RGO (CoTPP/RGO) nanocomposite. This composite was well characterized by scanning electron microscopy (SEM), fluorescence and UV-vis spectrometry. The electrochemical behavior of CoTPP/RGO for electrocatalytic dioxygen reduction was studied on the surface of glass carbon electrode (GCE) modified with the composite by cyclic voltammetry (CVs). When the mass ratio of RGO to CoTPP is 1:1 in the composite, CoTPP/RGO film displayed superb electroreduction of oxygen.

Keywords: cobalt meso-tetraphenylprophyrin (CoTPP); reduced graphene oxide (RGO); nanocomposite; electrocatalytic dioxygen reduction

1. INTRODUCTION

Graphene, a two-dimensional sheet made up by sp^2 conjugated carbon atoms, can be regarded as a versitle polyaromatic platform for functional materials owing to its open ended structure [1]. This two-dimensional carbon material has been utilized as a general stuff for all other graphitic materials [2]. It poses excellent electrochemical properties by virtue of its large surface area, extraordinary electron transport property, exceptional electrocatalytic activity, good mechanical strength, high thermal conductivity and excellent charge mobility [3-7]. These special characters turn graphene into a promising additive or supporting component for improving performance of various materials such as

photovoltaic cell [8,9], lithium-ion battery [10,11], ultracapacitor cell [12], biosensor [13], fuel cell [14] and so on.

Porphyrin compounds have aromaticity, good stability, wide spectral response and powerful complexing ability with metal ion. Cobalt porphyrins, metalloporphyrin derivatives, were usually acted as oxygen carriers for oxygen transport. To date, graphene-based nanomaterials have attracted unquestionable interest for their application in electrochemical sensors and biosensors. Graphene nanocomposites have also become a focused subject of materials because they provide ability to improve the material function [15], and the nanocomposites open the access to improve their electrochemical properties. It was disclosed that graphene-supported nanoparticles greatly promoted some electrochemical reactions of small molecules which lead to the better electrochemical sensor [16-18]. In recent years, the porphyrin (metal porphyrin) graphene composite materials have been synthesized by covalent bond, π-π stacking and electrostatic attraction [19,20]. Metal porphyrin-graphene nanocomposites for oxygen and the other reactions have been researched. In the paper, we have synthesized cobalt meso-tetraphenylprophyrin-reduced graphene oxide (CoTPP/RGO) and demonstrated this nanocomposite modified on the surface of electrode possesses the powerful ability for the catalytic oxygen reduction.

2. EXPERIMENTAL

2.1 Reagents

All reagents used in this work were of analytical grade and employed without further purification. Graphite was purchased from Sinopharm Chemical Reagent Co. (Shanghai, China). Benzaldehyde, propionic acid, pyrrole and hydrazine solution (85%) was provided by Beijing Chemicals Inc (Beijing, China). Unless otherwise stated, all solutions were prepared with double-distilled water.

2.2 Apparatus

UV-vis absorbance measurements were carried out on Lambda 35 (Perkin-Elmere, USA). Fluoroscence spectra were recorded with a Shimadzu RF-5301PC Fluorescence Spectrophotometer (Shimadzu, Japan). Electrochemical measurements was conducted on a CHI 832 Electrochemical workstation (CHI, USA). The morphologies of RGO and CoTPP/RGO were examined with a JSM-671F cold field emission scanning electron microscope (SEM, Electro-optical company, Japan). Acidity was measured by a PHS-3B Precision pH Meter (Shanghai, China), and all sonication was done using a KQ-100 Ultrasonic Cleaner (Kunshan, China).

2.3 Preparation of RGO

Graphene oxide (GO) was prepared from graphite by a revised Hummers method [21,22]. Hydrazine hydrate was added into GO drop by drop, and then reacted at 80℃ for 24h. After cooling the mixture to room temperature, the obtained solid was filtered, followed by washing with methanol and distilled water, and dried to get RGO.

2.4 Preparation of CoTPP

According to the previous literature, CoTPP was synthesized [23]. The mixture of 7.5 mL benzaldehyde and 200 mL propionic acid were slowly added to the mixture of 5 mL pyrrole and 10 mL propionic acid, and then refluxed for 1h. Cooling to room temperature, 5 mL ethanol was added. After standing for 8h, the solid was filtered, followed by washing with methanol and propionic acid, and lastly dried at 80℃ under vacuum. The mixture of 15 mL chloroform and 15 mL DMF (fresh distillation) was added to the obtained 100 mg TPP, and then stirred for 10 min. The mixture was added 1.0 g $CoCl_2$ and heated with stirring for 1h. The obtained mixture was added distilled water and extracted with chloroform for several time, and the extract was dried by anhydrous $MgSO_4$. The pure CoTPP was obtained by column chromatography.

2.5 Preparation of CoTPP/RGO

Dichloromethane as the solvent, 5 mg/mL CoTPP solution and 5 mg/mL RGO suspension was prepared, and then mixture. During ultrasonication, ethanol is added dropwise until the liquid became clear. The nanocomposite was gained by filtration, washed with water and ethanol, and dried in vacuum (80℃).

2.6 Modification of the electrode

Before any modification, the glass carbon electrode (GCE) was polished with 1.0, 0.3 and 0.05 μm alumina slurry, rinsed thoroughly with ultrapure water and ethanol, dried with nitrogen, then washed successively with 1:1 nitric acid, acetone, and ultrapure water in an ultrasonic bath and dried in air. 1 mg CoTPP/RGO nanocomposite was dispersed in 1 mL DMF under ultrasonication for 1 h. A few suspended droplets was added to the polished GCE surface, and then dried at room temperature.

2.7 Electrochemical measurement

Cyclic voltammetry measurements (CVs) were carried out with a CHI 832 electrochemistry workstation in 0.1 M different pH solution with a conventional three-electrode system comprised of a platinum wire as the auxiliary electrode, an Ag/AgCl as the reference electrode and the modified GCE as working electrode at a appropriate potential range.

3. RESULTS AND DISCUSSION

3.1 Characterization of CoTPP/RGO nanocomposite

The morphology of RGO and CoTPP/RGO nanocomposites were characterized by scanning electromicroscopy (SEM). Fig. 1A shows the typical layered RGO sheets like flake randomly packed in stacked structures, which illustrated that graphene sheet was formed. Furthermore, the adsorption of CoTPP on the RGO surface could be clearly observed in SEM image and this indicated a homogenous film was obtained. We think π-π interaction between RGO sheets and CoTPP molecules might account for forming this composite. As shown in Fig. 1B, the layered and wrinkled CoTPP film resides on the surface of the RGO sheets. Compared to the morphology of pure RGO, the layered composites look rougher. The image of CoTPP/RGO reveals that the CoTPP/RGO nanocomposites generate. Owing to a large surface area, CoTPP/RGO nanocomposites could be utilized for facile immobilization of various catalysts.

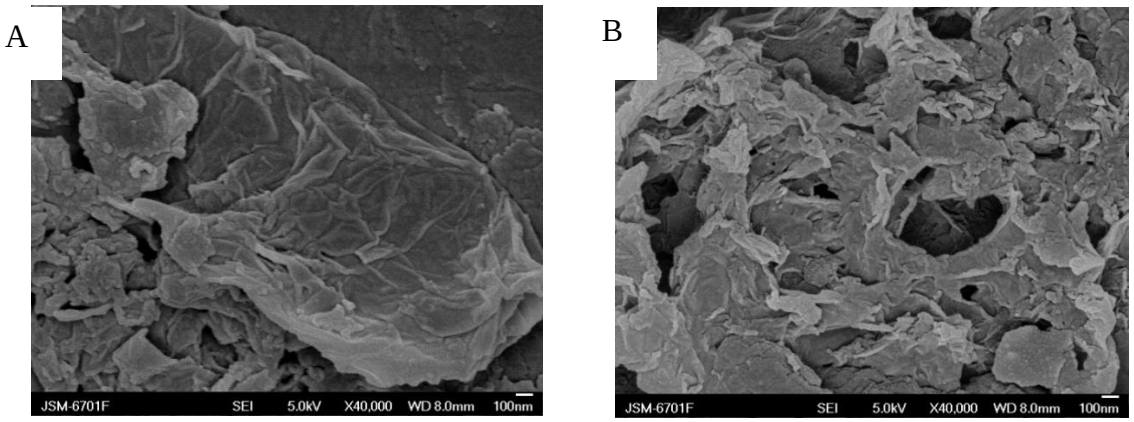

Figure 1. SEM images of RGO (A) and CoTPP/RGO (B).

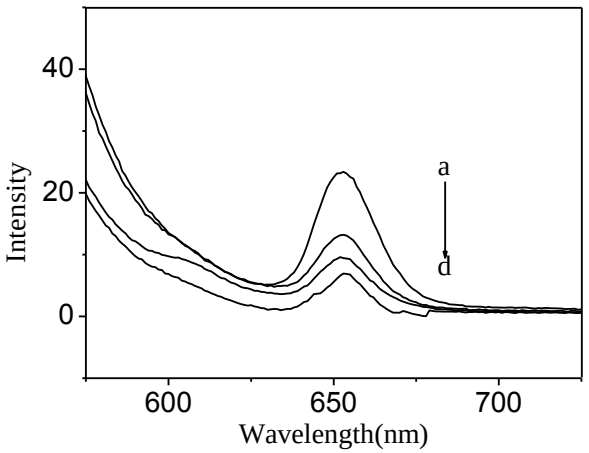

Figure 2. Fluorescence spectra of CoTPP(a) and CoTPP/RGO composites, the mass ratio of CoTPP and RGO in composite is 10:1(b), 1:10(c), 1:1(d).

The electronic interactions of CoTPP and RGO were studied by fluorescence spectra of CoTPP/RGO composites (Fig. 2). CoTPP has a strong fluorescence peak at 653nm. When CoTPP combines with RGO, the remarkble luminescence quenching of CoTPP reveals a strong interaction between the excited state of CoTPP and RGO. Photoinduced electron transfer or energy transfer from the excited state of CoTPP to the RGO may account for the above quenching and in this process RGO sinks charges with its conjugated network. This is a further evidence for formation of CoTPP/RGO composites. By comparsion, the quenching is extremely obvious when mass ratio of CoTPP and RGO in composite is 1:1. This is consistent with the former report [19,24-26]

Further evidence for the interaction between CoTPP and RGO was provided by UV–vis spectroscopic analysis. The data of UV–vis as shown in table 1, the spectrum of CoTPP in choloform solution displayed a strong absorbtion at 412nm, which is attributed to porphyrin soret-band. A weak band in the longer wavelength ascribed to the Q-band of porphyrin. However, after CoTPP interacts with the RGO, it is obvious that the absorption peak of porphyrin shifts from 412nm to 449nm for soret-band and from 548nm to 571nm for Q-band, which was attributed to the π–π stacking interaction between CoTPP and RGO. This was also consistent with the former report [27].

Table 1. The data of UV-vis characterization for CoTPP and CoTPP/RGO

Sample	Soret /λ(nm)	Q /λ(nm)
CoTPP	412 (2.15)	548 (0.18)
CoTPP/RGO	449 (1.17)	571 (0.07)

3.2. Electrochemical behaviors of CoTPP/RGO

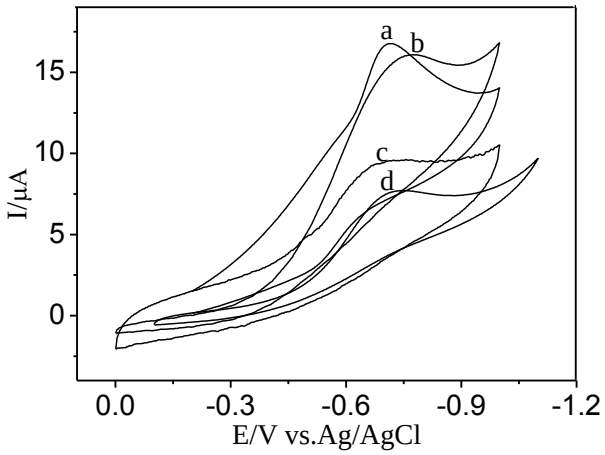

Figure 3. CVs of CoTPP/RGO/GCE (a), CoTPP/GCE (b), RGO/GCE (c) and bare GCE (d) in 0.1M NaAc-HAc buffer solution (pH=4.0) containing saturation oxygen, dispensing volume is 5μL, scan rate is 50 mV/s.

Cyclic voltammetry (CVs) was employed for investigating the electrochemical behavior of molecular oxygen at different electrodes. In 0.1M NaAc-HAc buffer solution (pH=4.0), it can be seen that CoTPP/RGO/GCE, CoTPP/GCE, RGO/GCE and bare GCE all represent electrocatalytic activity to dioxygen reduction (Fig. 3). The enhancement of these materials on the peak current of dioxygen reduction were CoTPP/RGO/GCE>CoTPP/GCE>RGO/GCE>bare GCE. The extraordinary electrocatalytic ability of CoTPP/RGO nanocomposite for dioxygen reduction were possibly attributed to their superior properties such as high surface area and electron conductivity which make their electron transfer rate increase significantly.

Numerous studies reported the graphene-supported porphyrins (phthalocyanines) or their metal compounds as efficient electrocatalysts for dioxygen reduction [28-32]. These nanocomposites revealed different electrocatalytic activity towards dioxygen reduction. In alkaline medium, almost all electrocatalysts established a pathway of 4-electron transfer reactions. But the preparation of these nanocomposites was complicated compared with our complex which is synthesized by the simple π-π conjugate interaction and can greatly improve the electrocatalytic activity of CoTPP combined with RGO.

3.3. Selection of optimization condition

Fig. 4 shows the CVs of the CoTPP/RGO/GCE in 0.1M NaAc-HAc buffer solution (pH=4.0) containing saturation oxygen with different mass ratio of CoTPP and RGO in composite. It can be seen that dioxygen reduction peak potential for different mass ratio remains unchanged basically. By comparison, the more obvious changes is current intensity. Under the mass ratio of CoTPP and RGO in composite is 1:1, it can be observed that the reduction peak currents of dioxygen achieved the largest. It may be due to the CoTPP can be dispersed uniformly and did not gathered at graphene surface, which promote the electron transfer effectively under this mass ratio.

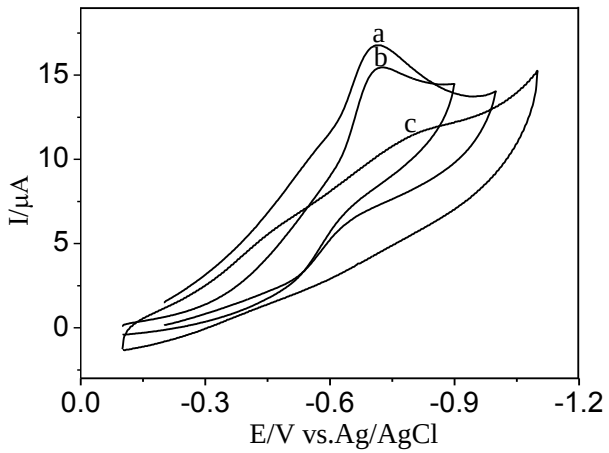

Figure 4. CVs of CoTPP/RGO/GCE in 0.1M NaAc-HAc buffer solution (pH=4.0) containing saturation oxygen with different mass ratio of CoTPP and RGO in composite: (a) 1:1, (b) 1:10 and (c) 10:1, dispensing volume is 5μL, scan rate is 50 mV/s.

The reduction peak currents are directly related to the amount of CoTPP/RGO deposited on glassy carbon electrode. When 5μL CoTPP/RGO suspension is deposited on the surface of GCE and the concentration of CoTPP/RGO is 1 mg/mL, the reduction peak current and peak potential of dioxygen reach optimal (Fig. 5). When the volume of CoTPP/RGO is greater than 5μL, CoTPP/RGO coating on electrode surface becomes excessively thick. The excessive thick CoTPP/RGO coating inhibits the diffusion of catalytic substrate to electrode surface and the result is the catalyst can not work efficiently. Thus the reduction peak current is reduced and the peak potentials is more negative.

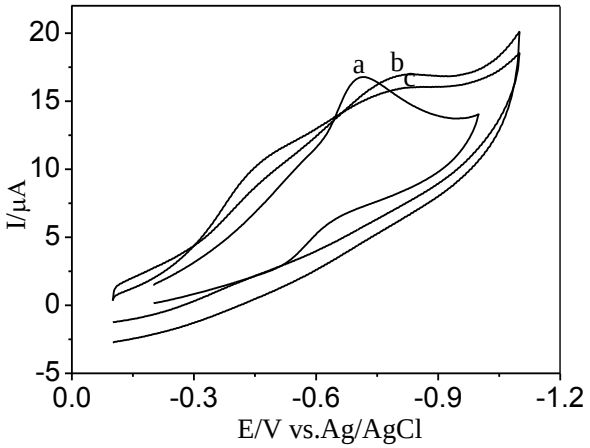

Figure 5. CVs of CoTPP/RGO/GCE in 0.1M NaAc-HAc buffer solution (pH=4.0) containing saturation oxygen with different dispensing volume. (a) 5μL, (b) 10μL and (c) 3μL, mass ratio of CoTPP and RGO in composite is 1:1, scan rate is 50 mV/s.

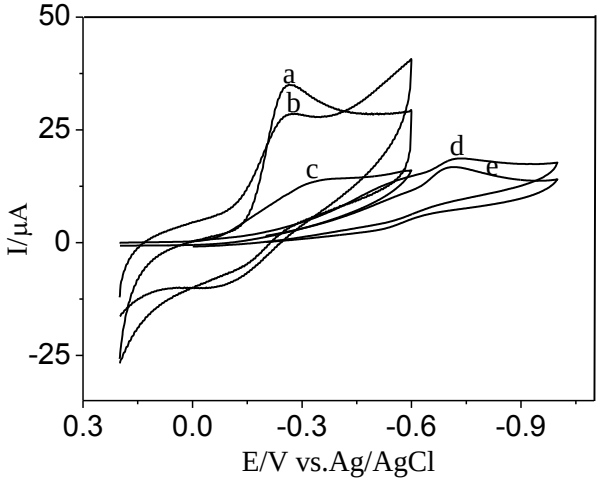

Figure 6. CVs of CoTPP/RGO/GCE in the presence of saturation oxygen with different pH solution (0.1M): (a) pH 12.0, (b) pH 10.0, (c) pH 7.0, (d) pH 4.0 and (e) pH 1.0, mass ratio of CoTPP and RGO in composite is 1:1, dispensing volume is 5μL, scan rate is 50 mV/s.

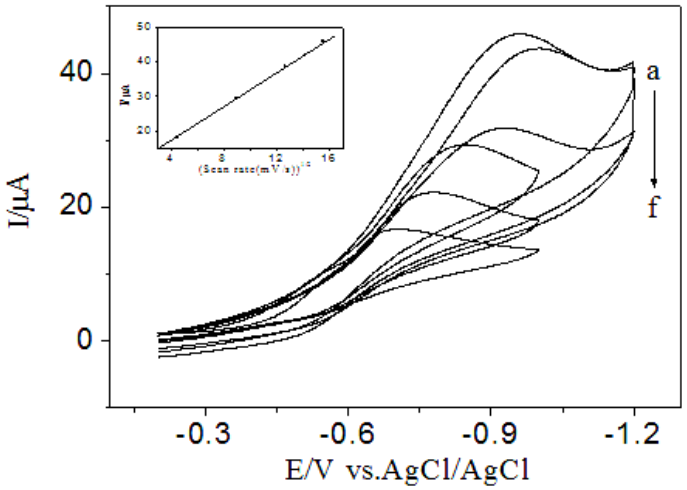

Figure 7. CVs of CoTPP/RGO/GCE on different scan rate in the presence of saturation oxygen (0.1M H_2SO_4, pH=1.0) (a-**Error! Reference source not found.**f): 240, 200, 160, 80, 40, 20 mV/s, insert: current intensity vs $v^{1/2}$.

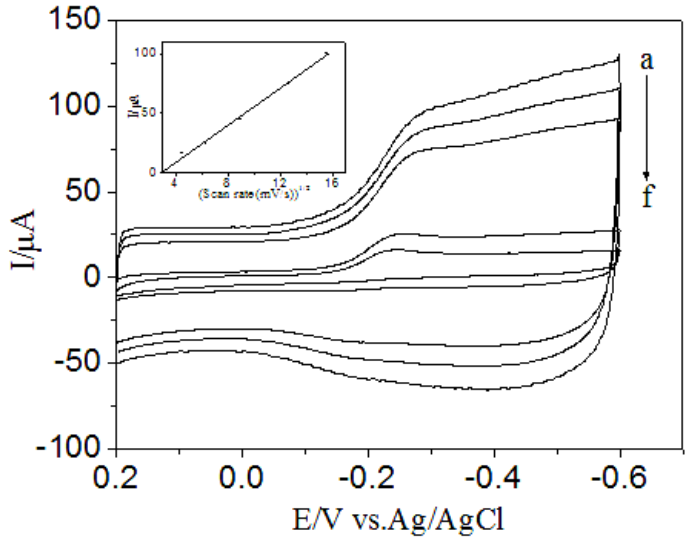

Figure 8. CVs of CoTPP/RGO/GCE on different scan rate in the presence of saturation oxygen (0.1M NaOH, pH=12) (a**Error! Reference source not found.**f): 240, 200, 160, 80, 40, 20 mV/s, insert: current intensity vs $v^{1/2}$.

Moreover, when the casting volume of CoTPP/RGO is less than 5μL, the catalyst can not cover fully on the surface of electrodes, also cause the reduction peak current of dioxygen reduced. So, in our experiments, 5 μL of CoTPP/RGO suspension with a concentration of 1 mg/mL was used in the preparation of CoTPP/RGO-modified electrode. Fig. 6 shows the CVs of CoTPP/RGO/GCE in the presence of saturation oxygen with different pH of buffer solution. Under acidic conditions, the reduction peak potential (about -0.7V) is more negative than neutral solution. Conversely, the

reduction peak potential (about -0.25V) is more positive in alkaline. In addition, the difference of reduction peak current is also greater in alkaline.

The electrochemical behavior of dioxygen reduction in different buffer solution (pH) under different scan rate were also investigated by CVs (Fig. 7 and 8). As scan rate in the range of 20 mV/s to 240 mV/s, the reduction peak intensity increased continuously. The relationship between current strength increased and square root of scan rate is linear. The regression equations is $I_{pc}=2.34v^{1/2}-7.47$ (μA, mV/s, R=0.70) in 0.1M H_2SO_4 solution (Fig. 7) and $I_{pc}=7.92v^{1/2}-24.99$ (μA, mV/s, R=0.60) in 0.1M NaOH solution (Fig. 8), respectively. This suggested that the electrocatalytic processes were controlled by molecular oxygen diffusion [33]. For a typical irreversible reaction, the relationship between peak current and scan rate was as follows [34-36].

$$i_p = 0.4958nFAC_0\left(\frac{\alpha n_\alpha F}{RT}\right)v^{\frac{1}{2}}D_0^{\frac{1}{2}} \qquad (1)$$

$$\Delta E_p = \frac{1.15RT}{\alpha n_\alpha F} \qquad (2)$$

∆**Error! Reference source not found.Error! Reference source not found.**E_p is the peak potential change when the scan rate increases 10-fold. The number of electrons n for the reduction of dioxygen is calculated as 1.89 when CoTPP/RGO/GCE is in 0.1M H_2SO_4 and 4.24 in 0.1M NaOH. It can be concluded that dioxygen reaching the surface of electrode by diffusion using CoTPP/RGO as catalyst was reduced mainly through a two-electron process to H_2O_2 in 0.1M H_2SO_4 solution, and a four-electron process to OH^- in 0.1M NaOH solution,. Electron transfer process was concerned with proton in acidic condition. Conversely, the oxygen can reduced easily under alkaline condition. And molecules oxygen were reduced directly to OH^- by acquirement of the four electrons. The reduction equation as follows.

$$O_2 + 2e^- + 2H^+ \rightarrow 2H_2O_2 \qquad (0.1\ \text{M}\ H_2SO_4)$$

$$O_2 + 4e^- + 2H_2O \rightarrow 4OH^- \qquad (0.1\ \text{M NaOH})$$

4. CONCLUSIONS

In summary, a new type of CoTPP-functionalized RGO nanocomposite was synthesized by simple π-π conjugate interaction. When modified these composites on the surface of GCE, the catalysis for oxygen reduction was investigated by CVs. When the mass ratio of CoTPP and RGO in composite is 1:1, catalytic efficiency of this nanocomposite for dioxygen reduction is optimal. Due to the feature of high stability, catalytic efficiency, low pollution, CoTPP/RGO nanocomposites materials can be useful for electrochemical catalytic performance.

ACKNOWLEDGEMENTS
This work was supported by the Natural Science Foundation of China (No. 21465021, 21463023), the Key Project of Chinese Ministry of Education (No. 211189), the Natural Science Foundation of Province of Gansu, China (No. 1208RJZE139), the "QingLan" Talent Engineering Funds of Tianshui Normal Universiy and the Program of Gansu Provincial University for Leaders of Disciplines in Science, China (No. 11zx-04).

References

1. C. N. R. Rao, A. K. Sood, K. S. Subrahmanyam, A. Govindaraj, Angew Chem Int.Ed 48 (2009) 7752.
2. K. P. Loh, Q. L. Bao, P. K. Ang, J. X. Yang, J Mater Chem 20 (2010) 2277.
3. S. Guo, S. Dong, Chem Soc Rev 40 (2011) 2644.
4. Y. Shao, J. Wang, H. Wu, J. Liu, I. A. Aksay, Y. Lin, Electroanal 22 (2010) 1027.
5. M. Pumera, A. Amborosi, A. Bonanni, E. L. K. Chng, H. L. Poh, Thrends Anal Chem 29 (2010) 954.
6. S. Guo, D. Wen, Y. Zhai, S. Dong, E. Wang, ACS Nano 4 (2010) 3959.
7. Y. Fang, S. Guo, C. Zhu, Y. Zhai, E. Wang, Langmuir 26 (2010) 11277.
8. T. Umeyama, H. Imahori, J Phys Chem C 117 (2013) 3195.
9. G. D. Sharma, D. Daphnomili, K. S. V. Gupta, T. Gayathri, S. P. Singh, P. A. Angaridis, T. N. Kitsopoulos, D. Tasise, A. G. Coutsolelos, RSC Adv 3 (2013) 22412.
10. M. Srivastava, J. Singh, T. Kuila, R. K. Layek, N. H. Kime, J. H. Lee, Nanoscale 7 (2015) 4820.
11. J. X. Zhu, D. Yang, Z. Y. Yin, Q. Y. Yan, H. Zhang, small 10 (2014) 3480.
12. W. X. Song, X. B. Ji, W. T. Deng, Q. Y. Chen, C. Shen, C. E. Banks, Phys Chem Chem Phys 15 (2013) 4799.
13. X. H. Deng, H. Tang, J. H. Jiang, Anal Bioanal Chem 406 (2014) 6903.
14. Y. Zheng, Y. Jiao, M. Jaroniec, Y. G. Jin, S. Z. Qiao, Small 8 (2012) 3550.
15. J. P. Yang, P. C. Huang, J Appl Polym Sci 77 (2000) 484.
16. S. Guo, D. Wen, Y. Zhai, S. Dong, E. Wang, ACS Nano 4 (2010) 3959.
17. H. Chang, X. Wu, C. Wu, Y. Chen, H. Jiang, X. Wang, Analyst 136 (2011) 2735.
18. F. Xu, Y. Sun, Y. Zhang, Y. Shi, Z. Li, Electrochem. Commun 13 (2011) 1131.
19. N. Karousis, A. S. D. Sandanayaka, T. Hasobe, S. P. Economopoulos, E. Sarantopoulou, N. Tagmatarchis, J Mater Chem 21 (2011) 109.
20. L. Wu, L.Y. Feng, Biosens. Bioelectron 34 (2012) 57.
21. Z. Jin, D. Nackashi, W. Lu, C. Kittrell, J. M. Tour, Chem Mater 22 (2010) 5695.
22. H. A. Becerril, J. Mao, Z. F. Liu, R. M. Stoltenberg, Z. N. Bao, Y. S. Chen, ACS Nano 2 (2008) 463.
23. G. F. Zuo, H. Q. Yuan, J. D. Yang, R. X. Zuo, X. Q. Lu. J Mol Catal A-Chem 269 (2007) 46.
24. A. Wojcik , P. V. Kamat, ACS Nano 4 (2010) 6697.
25. Y. F. Xu, Z. B. Liu, X. L. Zhang, Y. Wang, J. G. Tian, Y. Huang, Y. F. Ma, X. Y. Zhang, Y. S. Chen, Adv Mater 21 (2009) 1275.
26. M. B. M. Krishna, N. Venkatramaiah, R. Venkatesan, D. N. Rao, J Mater Chem 22 (2012) 3059.
27. T. X. Ye, S. L. Ye, D. M. Chen, Q. A. Chen, B. Qiu, X. Chen, Spectrochim Acta A 86 (2012) 467.
28. L. Q. Jiang, M. Li, L. Lin, Y. F. Li, X. Q. He, L. L. Cui, RSC Adv 4 (2014) 26653.
29. L. L. Cui, G. J. Lv, X. Q. He, J Power Sources 282 (2015) 9.
30. S. K. Kim, S. Jeon, Electrochem Commun 22 (2012) 141.
31. J. M. You, H. S. Han, H. K. Lee, S. Cho, S. Jeon, Int J Hydrogen Energ 39 (2014) 4803.
32. V. Mani, R. Devasenathipathy, S. M. Chen, J. A. Gu, S. T. Huang, Renew Energ 74 (2015) 867.

33. W. Lu, C. Wang, Q. Lv, X. Zhou, J. Electroanal. Chem (2003) 558.
34. R. S. Nicholson, I. Shain, Anal Chem 36 (1964) 706.
35. A. J. Bard, L. R. Faulkner, Electrochemical Methods-Fundamentals and Applications, Wiley, New York, 1980 (chapters 3 and 12).
36. A. Fuerte, A. Cormab, M. Iglesias, E. Morales, F S'anchez, J Mol Catal A-Chem 246 (2006) 109.